Calculation of the Linear-Absorption Spectrum of an Ideal Two-Dimensional System of MoS_2

Presenter
Vo Chau Duc Phuong [1]

Supervisors
Dr. Huynh Thanh Duc [2]

[1]University of Science, Ho Chi Minh city

[2]Institute of Applied Mechanics and Informatics

February 23, 2025

Table of Contents

Transition Metal Dichalcogenide Monolayer

Transition metal dichalcogenide (TMD) is the compound has the form of MX_2.

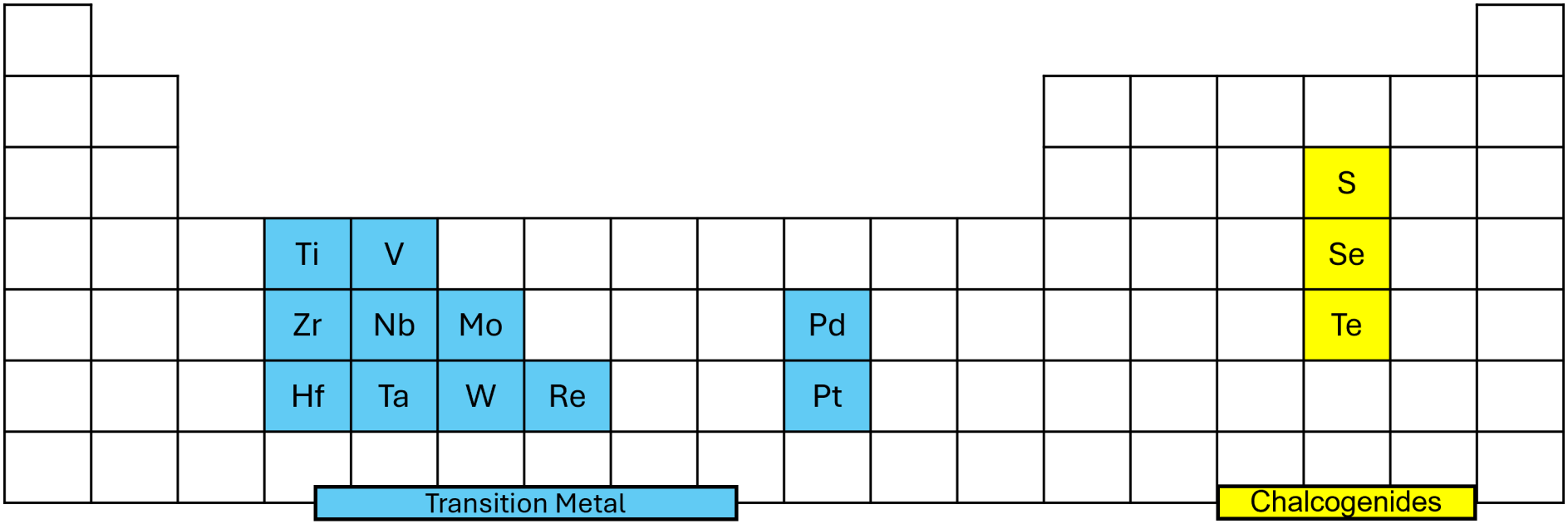

Figure: Transition metal dichalcogenide compound, M is a transition metal atom and X is a chalcogenides atoms

TMD Mono-layer structure

- The M (huge black dots) layer has been sandwiched by two X (small green dots) layers as shown in top view (a) and side view (b).
- They have the inverse asymmetry.
- The symmetry of the lattice results in the hexagon Brillouin Zone (BZ).

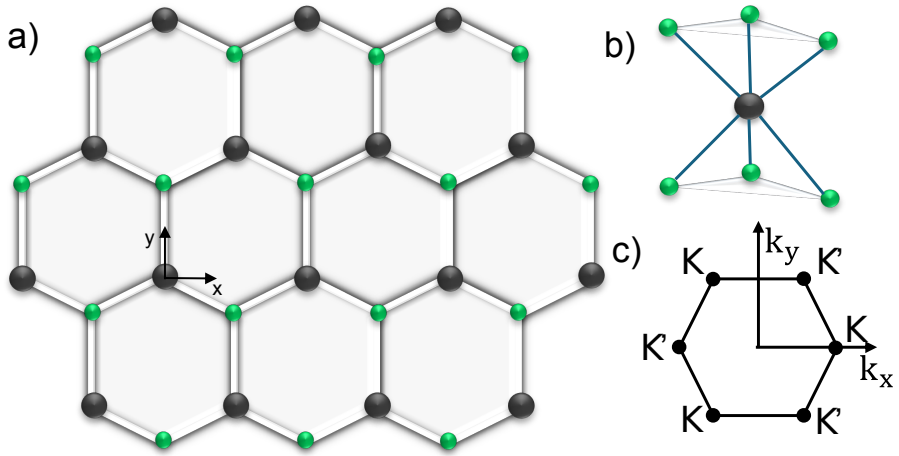

Figure: Structure and Brillouin Zone of Monolayer TMD, redrawing from[1]

My thesis focused on MoS_2 monolayer, has the visible band gap in the band structure, which can be used in creating the transistor devices.[2]

[1] Liu et al., "Three-band tight-binding model for monolayers of group-VIB transition metal dichalcogenides".

[2] Radisavljevic et al., "Single-layer MoS_2 transistors".

Splitting In The Band Structure

Huge split Δ (hundreds of meV) in valley (K and -K points) of the band structure caused by the strong spin-orbit coupling (SOC) and the inversion asymmetry.
$\Rightarrow$ Applications in spintronic and optoelectronics[3].

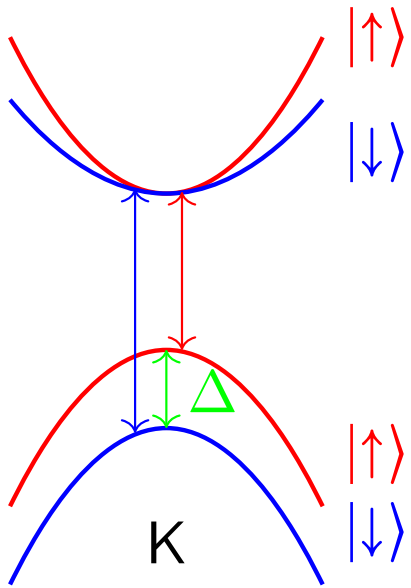

Figure: The allowed optical transition

[3] Liu et al., "Electronic structures and theoretical modelling of two-dimensional group-VIB transition metal dichalcogenides".

Binding Energy of Exciton

When an electron has been excited, it create a hole at initial position. Interaction between the electron and the hole call "Exciton".

$$-\left[\frac{\hbar^2\nabla^2_{\mathbf{r}}}{2m_r}+V(r)\right]\psi_\nu(\mathbf{r})=E_\nu(\mathbf{r})\psi_\nu(\mathbf{r}), \tag{1}$$

where,

- $V(r)$ is the Coulomb interaction with the form:

$$V(r)=\frac{e^2}{\varepsilon|\mathbf{r}|} \tag{2}$$

- $m_r=\frac{m_h m_e}{m_h+m_e}$ is the effective mass.
- $E_\nu(\mathbf{r})$ is the binding energy of the exciton.

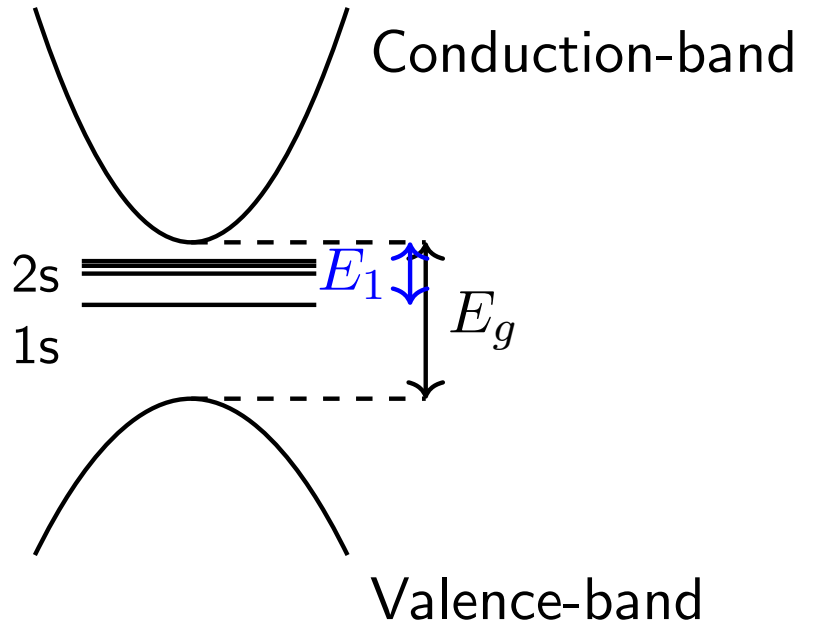

Figure: Binding energy relative to the band gap

Exciton

In the bulk crystals with relative small dielectric constant due to the screening, the exciton have the small binding energy.
Ex: GeAs[4]:

$$E_b \approx 4.8meV \ll E_g = 1.2 - 1.7eV$$

In these materials, the exciton binding energy can be neglected in simulations.

[4] Diakite et al., *Accurate Electronic, Transport, and Bulk Properties of Gallium Arsenide (GaAs)*.

Purpose

So, why need to calculate it in TMD?

- In the 2-D materials, lack of system dimension ⇒ decrease in the dielectric screening.

⇒ Increasing of exciton binding energy ~ 10^2 in compared with bulk semiconductor.

- Previous theories predict binding energy too large[5], experiment shows significant smaller[6].
- Find a model not only simple but also precise enough for further research and application.

⇒ Look like enough for my bachelor's thesis ☺.

---

[5] Ramasubramaniam, "Large excitonic effects in monolayers of molybdenum and tungsten dichalcogenides"; Qiu, Jornada, and Louie, "Optical Spectrum of $\mathrm{MoS_2}$".

[6] Zhang et al., "Absorption of light by excitons and trions in monolayers of metal dichalcogenide $\mathrm{MoS_2}$".

Second Quantization Hamiltonian

The second quantization Hamiltonian in basis of Bloch function $\{|\psi_{\lambda\mathbf{k}}\rangle\}$ for many electrons with light-matter interaction:

$$\begin{aligned} H =& H_{1e}^{0} + H^{Coul.} + H^{e-L} \\ =& \sum_{\lambda\mathbf{k}} \varepsilon_{\lambda}(\mathbf{k}) c_{\mathbf{k}}^{\dagger} c_{\mathbf{k}} + \frac{1}{2} \sum_{\mathbf{k}\mathbf{k}'\mathbf{q}} \sum_{\alpha\beta\gamma\delta} V_{\mathbf{k},\mathbf{k}',\mathbf{q}}^{\alpha\beta\gamma\delta} c_{\alpha\mathbf{k}+\mathbf{q}}^{\dagger} c_{\beta\mathbf{k}'-\mathbf{q}}^{\dagger} c_{\gamma\mathbf{k}} c_{\delta\mathbf{k}'} \\ &+ \sum_{\lambda\lambda'\mathbf{k}\mathbf{k}'} \langle\psi_{\lambda\mathbf{k}}| \frac{e}{m} \mathbf{A}(\mathbf{r},t).\mathbf{p} |\psi_{\lambda'\mathbf{k}'}\rangle c_{\lambda\mathbf{k}}^{\dagger} c_{\lambda'\mathbf{k}'} + \mathrm{O}(\mathbf{A}^2), \end{aligned} \tag{3}$$

in which the creation $c_{\lambda\mathbf{k}}^{\dagger}$ and annihilation $c_{\lambda\mathbf{k}}$ operator satisfied the anti-commutator relation[7]:

$$\{c_{\lambda\mathbf{k}}^{\dagger}, c_{\lambda'\mathbf{k}'}^{\dagger}\} = \{c_{\lambda\mathbf{k}}, c_{\lambda'\mathbf{k}'}\} = 0; \quad \{c_{\lambda\mathbf{k}}, c_{\lambda'\mathbf{k}'}^{\dagger}\} = \delta_{\lambda\lambda'}\delta_{\mathbf{k}\mathbf{k}'}$$

[7] $\{A,B\} = AB + BA$

The coulomb interaction matrix elements:

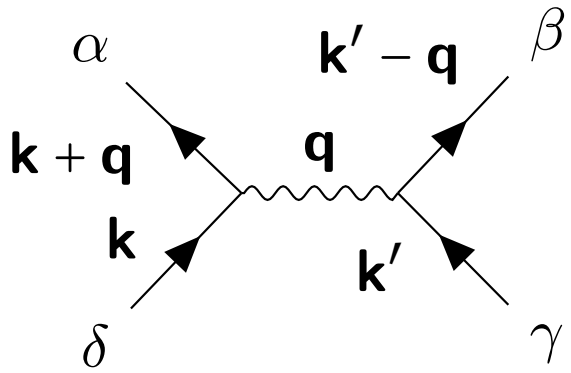

$$V^{\alpha\beta\gamma\delta}_{\mathbf{k},\mathbf{k'},\mathbf{q}} = \left\langle \psi_{\alpha\mathbf{k}+\mathbf{q}}\psi_{\beta\mathbf{k'}-\mathbf{q}} \right| V_{ee} \left| \psi_{\gamma\mathbf{k}}\psi_{\delta\mathbf{k'}} \right\rangle = \tag{4}$$

$$= \int \frac{d^3r}{V} \int \frac{d^3r'}{V} e^{-i\mathbf{q}(\mathbf{r}-\mathbf{r'})} u^*_{\alpha\mathbf{k}+\mathbf{q}}(\mathbf{r}) u^*_{\beta\mathbf{k}-\mathbf{q}}(\mathbf{r'}) V_{ee} u_{\gamma\mathbf{k'}}(\mathbf{r'}) u_{\delta\mathbf{k}}(\mathbf{r}),$$

With the 3-D Coulomb interaction have the form:

$$V_{ee}(\mathbf{r}) = \frac{e^2}{\varepsilon|\mathbf{r}|} \tag{5}$$

Using Fourier transform for the potential, apply long-wave approximation and take the limit $z \to 0$ to have the 2-D Coulomb matrix elements:

$$V^{\alpha\beta\gamma\delta}_{\mathbf{k},\mathbf{k'},\mathbf{q}} = \frac{e^2}{2\varepsilon L^2} \frac{1}{|\mathbf{q}_\parallel|} \left\langle u_{\alpha\mathbf{k}+\mathbf{q}} \middle| u_{\delta\mathbf{k}} \right\rangle \left\langle u_{\beta\mathbf{k'}-\mathbf{q}} \middle| u_{\gamma\mathbf{k'}} \right\rangle \tag{6}$$

Phenomenally characterize the scattering term:

$$\left(\frac{\mathrm{d}\rho(\mathbf{k})}{\mathrm{d}t}\bigg|_{scat.}\right)_{\lambda\lambda'} \to -\frac{\rho_{\lambda\lambda'}(\mathbf{k})}{T_2}(1-\delta_{\lambda\lambda'}) \tag{7}$$

The parameter T_2 can be chosen $\to$ fit with the experiments.

Finally, we have the semiconductor Bloch equations[8]:

$$\begin{aligned}\frac{\mathrm{d}\rho_{\lambda\lambda'}(\mathbf{k})}{\mathrm{d}t} =& \frac{i}{\hbar}(\varepsilon_\lambda(\mathbf{k}) - \varepsilon_{\lambda'}(\mathbf{k}))\rho_{\lambda\lambda'}(\mathbf{k}) \\ &- \frac{i}{\hbar}\sum_\mu \left(\Sigma_{\mu\lambda}(\mathbf{k}) \left\langle c^\dagger_{\mu\mathbf{k}} c_{\lambda'\mathbf{k}} \right\rangle - \left\langle c^\dagger_{\lambda\mathbf{k}} c_{\mu\mathbf{k}} \right\rangle \Sigma_{\mu\lambda'}(\mathbf{k}) \right) \\ &- \frac{\rho_{\lambda\lambda'}(\mathbf{k})}{T_2}(1 - \delta_{\lambda\lambda'}),\end{aligned} \tag{8}$$

where,

$$\Sigma_{\mu\nu} = \frac{e\mathbf{A}(t)}{m}\mathbf{p}_{\mu\nu}(\mathbf{k}) - \sum_{\alpha\beta\mathbf{q}} V^{\alpha\mu\beta\nu}_{\mathbf{k},\mathbf{k}+\mathbf{q},\mathbf{q}} \rho_{\alpha\beta}(\mathbf{k}+\mathbf{q}) \tag{9}$$

At $0K$, initial conditions at $(t = -\infty)$:

$$\rho_{\lambda\lambda'}(\mathbf{k}) = \delta_{\lambda v}\delta_{\lambda' v} \quad \forall \mathbf{k}$$

[8] Haug and Koch, *Quantum Theory Of The Optical And Electronic Properties Of Semiconductors (fifth Edition)*.

Three-band Tightbinding model

Using basic functions of d-type orbitals:

$$|\phi_1\rangle = d_{z^2}, |\phi_2\rangle = d_{xy}, |\phi_3\rangle = d_{x^2-y^2} \Rightarrow H^{TB}_{3\times3}(\mathbf{k})$$

Three-band TB Hamiltonian with SOC has the form[9]:

$$H^{TB}_{6\times6}(\mathbf{k}) = \begin{bmatrix} H^{TB}_{3\times3}(\mathbf{k}) + \gamma L_z & 0 \\ 0 & H^{TB}_{3\times3}(\mathbf{k}) - \gamma L_z \end{bmatrix}, \quad L_z = \begin{bmatrix} 0 & 0 & 0 \\ 0 & 0 & i \\ 0 & -i & 0 \end{bmatrix}.$$

[9] Liu et al., "Three-band tight-binding model for monolayers of group-VIB transition metal dichalcogenides".

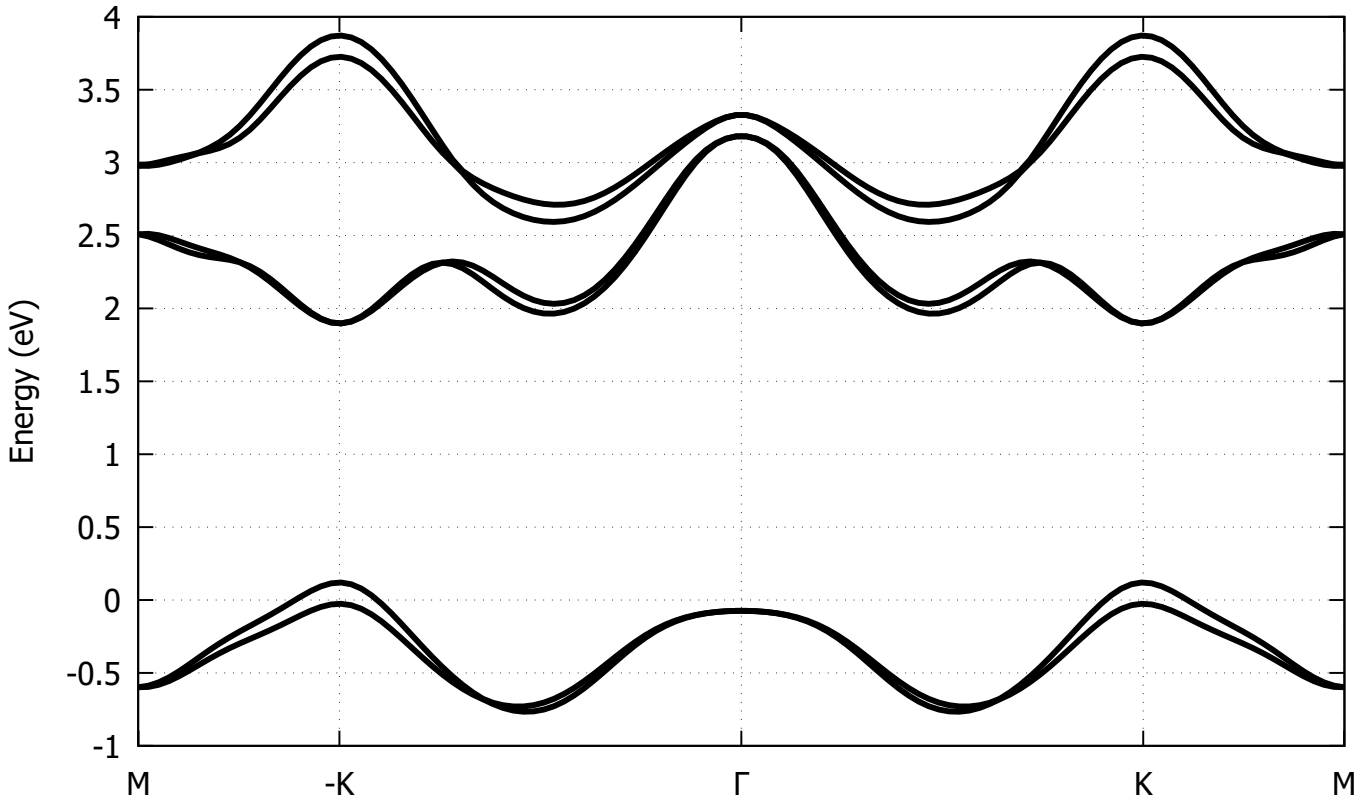

Figure: Band structure of MoS_2 monolayer

Numerical Evaluation of The Sum Over k-space

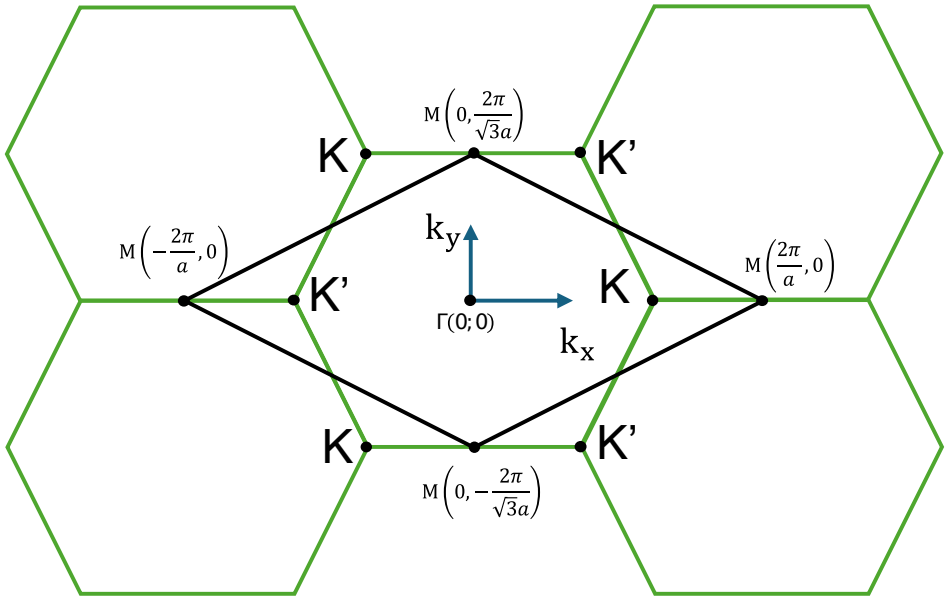

Figure: Rhombus primitive cell

$$\sum_{\mathbf{k}} ... \rightarrow \frac{L^2}{4\pi^2} \int \int_{BZ} dk_x dk_y ... \tag{10}$$

k-cutoff approximation method

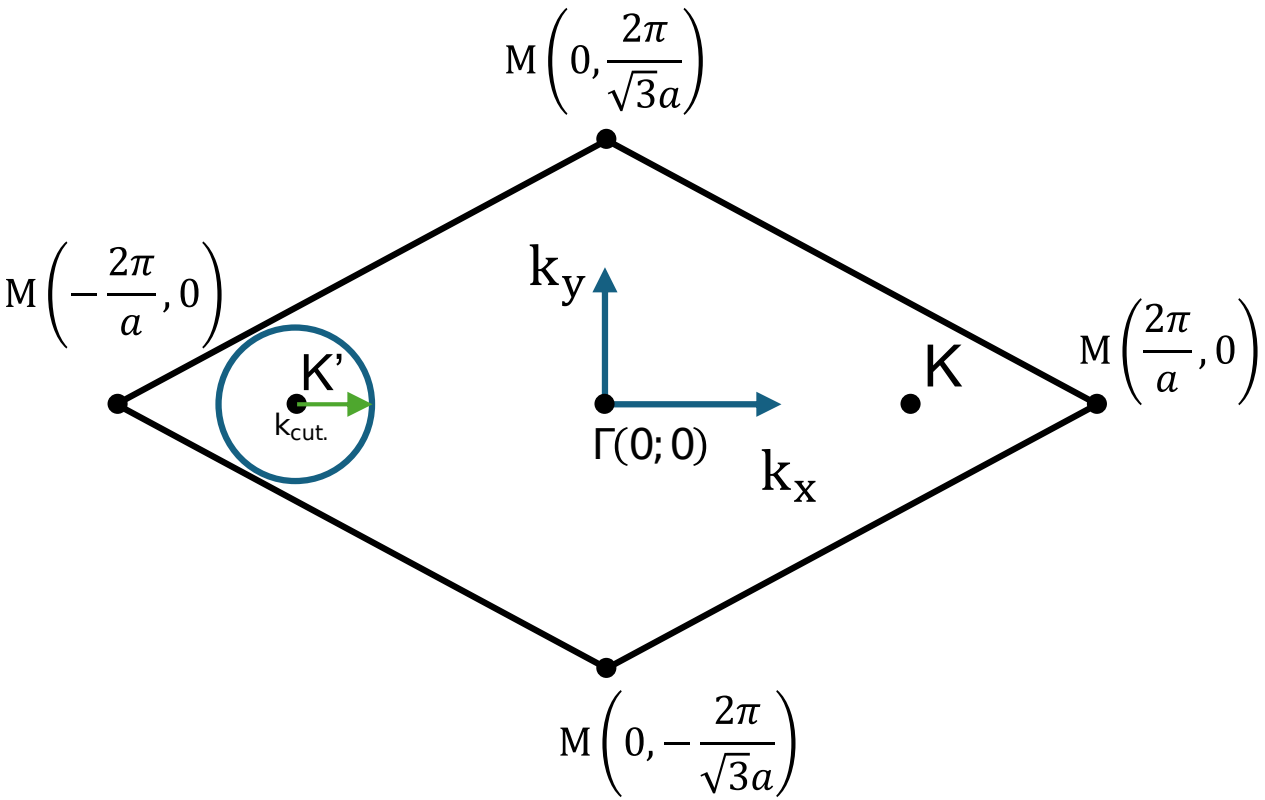

For k-points around **K'** point

$$W^{\alpha\mu\beta\nu}_{\mathbf{k},\mathbf{k}',\mathbf{q}} \approx W^{\alpha\mu\beta\nu}_{\mathbf{k},\mathbf{k}',\mathbf{q}} \theta(k_{cut.} - |\mathbf{k} - \mathbf{k}_{K'}|)\theta(k_{cut.} - |\mathbf{k}' - \mathbf{k}_{K'}|). \qquad (11)$$

The same for k-points around **K** point

Electromagnetic Field

The electric field has a Gaussian envelope form:

$$\mathbf{E}(t) = \mathbf{E}_0 \cos(\omega_0 t) e^{-\frac{t^2}{\tau_L^2}} \qquad (12)$$

- small $E_0 : \rho_{cc}(\mathbf{k}) \to 0$
- $\hbar\omega_0 = E_{gap.}$
- small $\tau_L \to$ rounder Fourier transform's peak around ω_0

In numerical solving, choose time step Δt

$$\Delta t \ll \tau_L$$

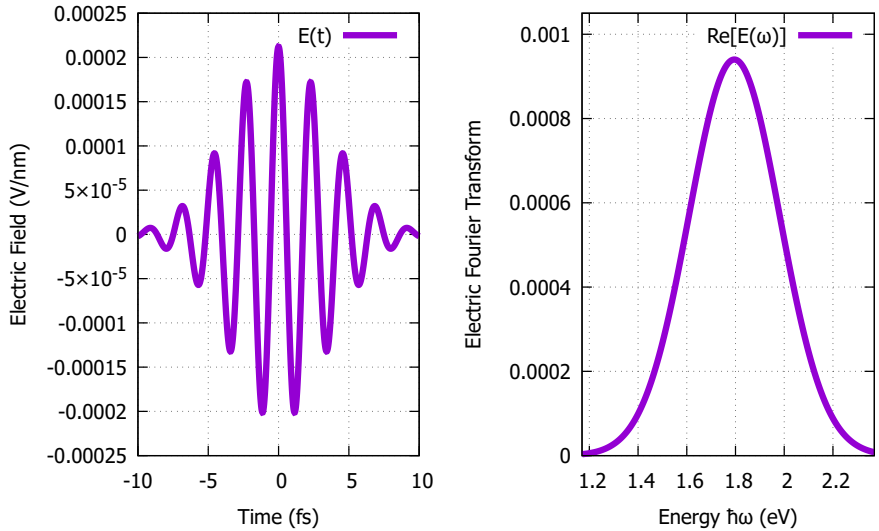

Figure: Electric field and it fourier transform

Absorption coefficient[10]:

$$\alpha(\omega) \propto \frac{P(\omega)}{E(\omega)}. \qquad (13)$$

[10] Haug and Koch, *Quantum Theory Of The Optical And Electronic Properties Of Semiconductors (fifth Edition)*.

Experiment measure:

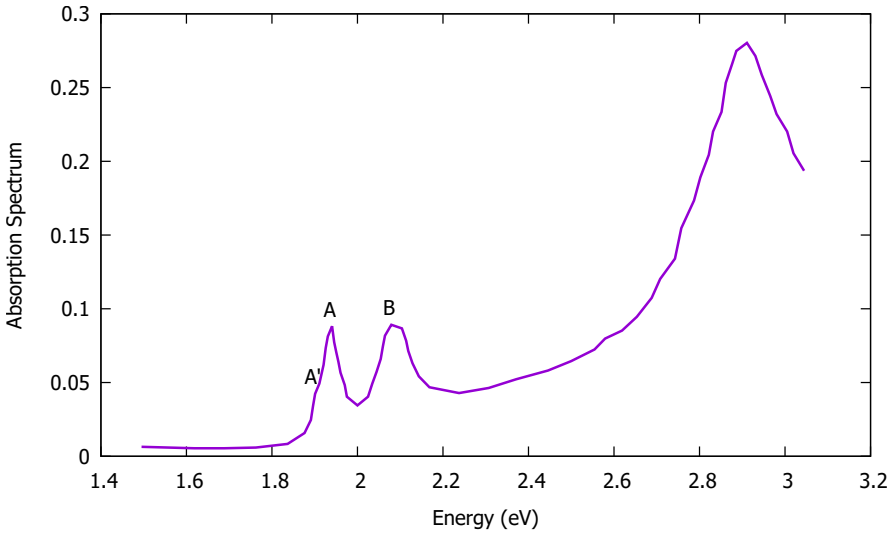

Figure: Measured Absorption Spectrum of MoS_2 at $T = 5K$ extracted from Ref.[11]

$$E_{gap} = 2.15 \pm 0.06\ eV$$

Binding energy:

$E_{bind.} = E_{gap} - E_A = 0.22\ eV$

From this figure, we see

- Two resonance labeled by A $(1.93\ eV)$ and B $(2.1\ eV)$ are exciton peaks (band split due to SOC)
- Weak trion peak near A labeled by A' $(18\ meV)$

To fit with experiment, we can change:

- Relative permittivity ε
- Dephasing time T_2

[11] Zhang et al., "Absorption of light by excitons and trions in monolayers of metal dichalcogenide MoS_2".

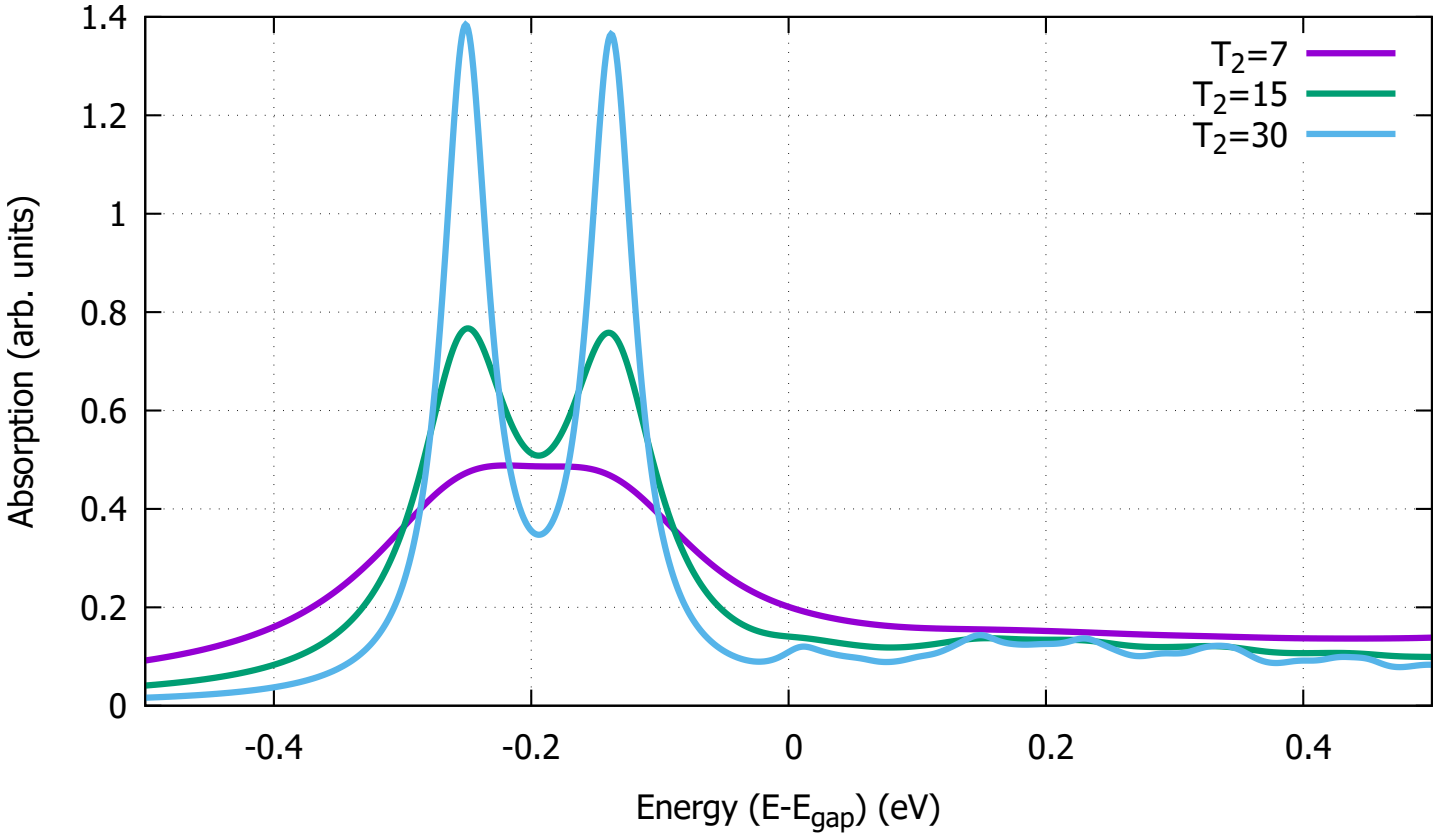

Choosing the T_2 for clearer Exciton peak:

- The bigger T_2, the clearer main Exciton peaks → confirm two peak.
- At $T_2 = 30\ fs$ show other smaller peaks → predict other peaks.

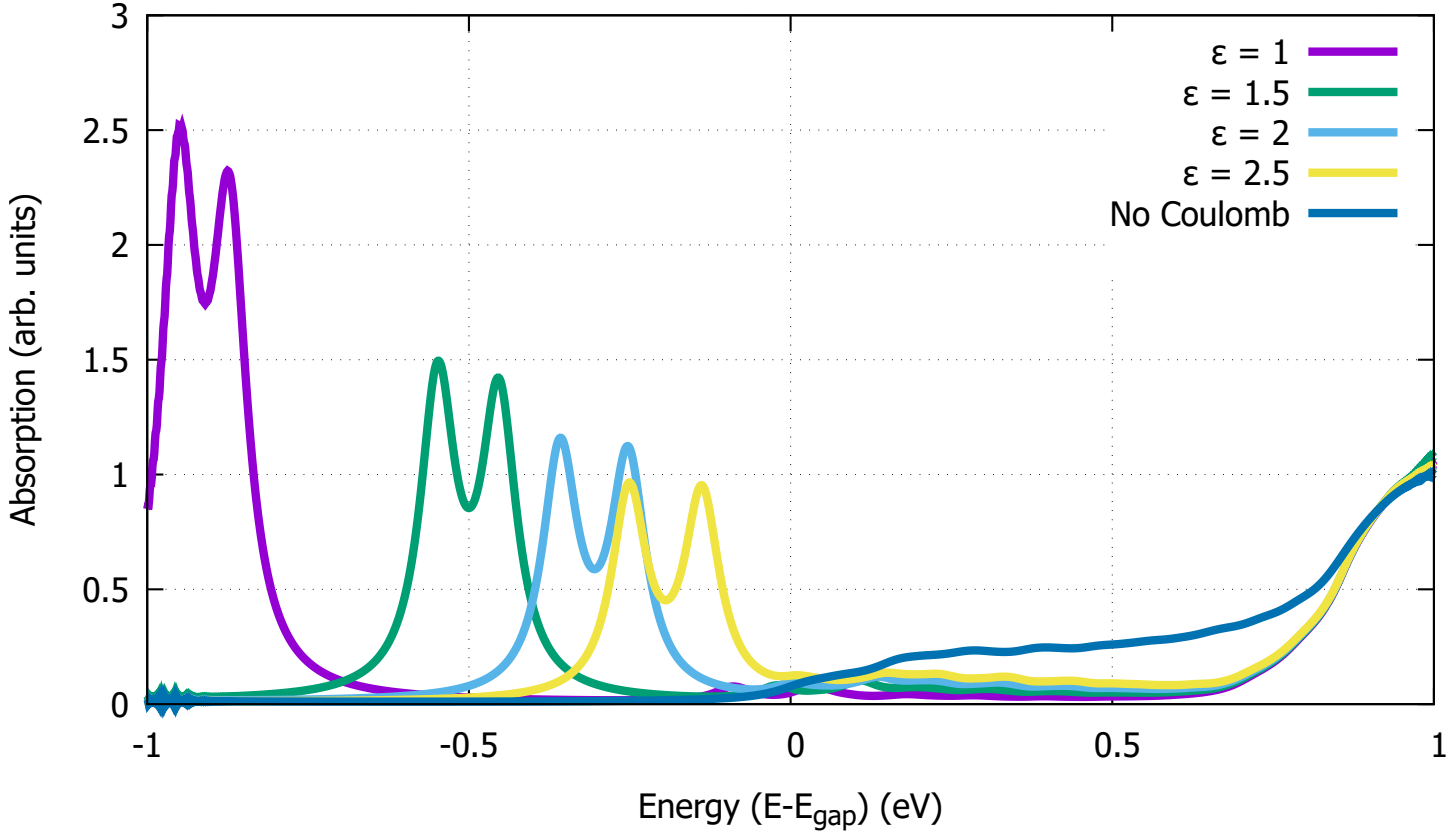

- Choosing the ε for fitting with the experiment.
- For the relative permittivity $\varepsilon \in (1.5, 2.5)$, binding energy is in good agreement with measurement $E_{bind.} = 0.2 - 0.5eV$[12]

[12] Zhang et al., "Absorption of light by excitons and trions in monolayers of metal dichalcogenide MoS_2".

Summary:

- From three-band TB + SBE → Linear Absorption Spectrum.
- We confirm the Exciton binding energy in this model is in agreement with experimental data, and predict smaller exciton peaks.

Further research:

- High Harmonic Generation
- High-order Side-band Generation
- Photovoltaic effect

Thank you for your listening.

For deeper calculation, source code, beamer e-pdf,... scan this.

- Ataca, C., H. Şahin, and S. Ciraci. "Stable, Single-Layer MX2 Transition-Metal Oxides and Dichalcogenides in a Honeycomb-Like Structure". In: (2012).
- Cheiwchanchamnangij, Tawinan and Walter R. L. Lambrecht. "Quasiparticle band structure calculation of monolayer, bilayer, and bulk MoS_2". In: *Phys. Rev. B* 85.20 (May 2012). Publisher: American Physical Society, p. 205302.
- Diakite, Yacouba Issa et al. *Accurate Electronic, Transport, and Bulk Properties of Gallium Arsenide (GaAs)*. 2016.
- Haug, Hartmut and Stephan W. Koch. *Quantum Theory Of The Optical And Electronic Properties Of Semiconductors (fifth Edition)*. en. Google-Books-ID: 1J1IDQAAQBAJ. Jan. 2009.
- Liu, Gui-Bin et al. "Electronic structures and theoretical modelling of two-dimensional group-VIB transition metal dichalcogenides". In: (2015).
- Liu, Gui-Bin et al. "Three-band tight-binding model for monolayers of group-VIB transition metal dichalcogenides". In: (2013).
- Qiu, Diana Y., Felipe H. da Jornada, and Steven G. Louie. "Optical Spectrum of MoS_2: Many-Body Effects and Diversity of Exciton